Materials Today: Proceedings xxx (xxxx) xxx

Contents lists available at ScienceDirect

Materials Today: Proceedings

journal homepage: www.elsevier.com/locate/matpr

Moisture diffusion affected by the Knudsen effect in temporal changing pore networks

Christoph Strangfeld [a,b,*], Heiko Stolpe [a], Philipp Wiehle [a]

[a] Bundesanstalt für Materialforschung und -prüfung, Unter den Eichen 87 12205, Berlin, Germany
[b] Hermann-Föttinger-Institut, Technische Universität Berlin, 10623, Berlin, Germany

ARTICLE INFO

Keywords:
Earth material
Material moisture
Physisoprtion
Chemisorption

ABSTRACT

Almost all building materials in civil engineering have an open porosity and interact with or are affected by the environmental conditions. Structures might suffer from effects such as moisture adsorption, carbonation, corrosion, penetration of salt ions and chemical substances, etc. In the hygroscopic range, these processes are mostly driven by diffusion. Due to the confinement of small pores (less than1 μm), the Knudsen effect reduces the molecular diffusion. This reduction can become more significant in case of temporal changing pore systems because of physisorption of water vapor, carbonation, or chemisorption.

In this study, unstabilised earth blocks and earth masonry are investigated. In a first step, the pore size distribution of the blocks is measured and sorption isotherms are recorded in experiments. Besides the ordinary physisorption, the involved clay minerals undergo swelling or shrinking due to chemisorption. The following two effects must be considered: first, the reduction of the available pore space by the adsorbed water layer. For this, the Hillerborg sorption theory is used, which is a combination of the well-known Brunauer-Emmett-Teller sorption theory and the Kelvin equation. This allows the computation of adsorbed water layers even in curved pore geometries. Second, the variation of the initial pore size distribution due to chemisorption needs to be modelled. Based on these two models, the effective diffusion coefficient can be predicted. For validation, arrays of relative humidity sensors were embedded into a free-standing earth masonry wall. This monitoring was carried out over more than a year to have a broad variety of environmental conditions and was located in Berlin, Germany.

The prediction of the effective diffusion coefficient can also be transferred to other processes and allows the investigation of materials having temporarily changing pore systems. Examples are the carbonation of cementitious materials, alkali silica reaction, calcium leaching of long-lasting structures, etc. These effects are prominent in the *meso*-pore range and might significantly alter the effective diffusion coefficient.

1. Motivation

The utilisation of load-bearing earth masonry can contribute to a significant reduction of the environmental impact caused by the building industry [1,2]. Earthen building materials generate less CO_2 than hydraulically binding cementitious materials and consume less primary energy than fired ceramic materials. The resources, especially the mineral aggregates, can be recycled and reused entirely in contrast to concrete or masonry rubble, which is used as filling material in road construction or other inferior processes. However, the load-bearing capacity of unstabilised earth masonry depends on its moisture content. If the material moisture increases, the mechanical performance decreases, which needs to be considered in the structural design [3,4]. Depending on whether the material is used as interior or exterior wall with or without insulation, the moisture content and its distribution throughout the wall's cross section will be inhomogeneous. In the case of conventional building materials, the moisture distribution and its variation can adequately be estimated using common Heat-Air-Moisture (HAM) simulations that are based on some physical simplifications like assuming an inert pore network and neglecting the sorption hysteresis which certainly does not apply in case of earthen materials. Especially the clay fraction and the content of organic matter cause volumetric changes like swelling and shrinking [5,6]. A prediction of the moisture content with existing models is questionable. Contrary to hydraulically hardening or

* Corresponding author.
E-mail addresses: christoph.strangfeld@bam.de (C. Strangfeld), philipp.wiehle@bam.de (P. Wiehle).

https://doi.org/10.1016/j.matpr.2023.09.034
Received 6 June 2023; Received in revised form 25 August 2023; Accepted 5 September 2023

fired materials, the moisture content of earthen materials is not only of interest in terms of building-physical performance but is a crucial aspect of the load-bearing capacity. As a result, the inhomogeneity of the moisture distribution needs to be considered in the structural design and therefore the moisture transport needs to be estimated adequately. Based on experimentally determined pore size distributions and water vapour sorption isotherms, the effective diffusion coefficient can be predicted employing Hillerborg's adsorption theory and considering the variation of the initial pore size and pore geometry. As the separation of chemisorption and physisorption is complex, a validation based on moisture monitoring of an earth masonry wall exposed to outdoor climate conditions will be a future step. However, a more precise prediction of moisture transport within porous material chemisorption will help to characterize and optimize new and more sustainable building materials.

2. Theory

2.1. Impact of moisture content on the mechanical properties of unstabilised earth masonry

The mechanical properties of unstabilised earth masonry decrease with increasing moisture content as shown in Fig. 1. More detailed information of the impact of the relative humidity (RH) on compressive strength and Youngs modulus of unstabilised earth blocks, mortars and masonry can be found in [1 4 7]. According to the evaluation of various studies by Brinkmann et al.[8], the reduction in both, compressive strength and Young's modulus, can be linearly correlated with the RH of the conditioning climate. Besides a reduction of compressive strength and Youngs modulus, an increase in axial strain at maximum stress can be observed. These results, however, are based on homogenously distributed moisture contents after storing the specimens in the respective climate until equilibrium is reached. Under real climate conditions, the moisture will be distributed inhomogeneously inside the wall's cross section. In accordance with Fick's law, surface-near areas will undergo adsorption or desorption much quicker than inner areas. Consequently, compressive strength and Youngs modulus, are varying throughout the cross section. An accurate description and determination of the inhomogeneities are therefore needed to ensure sufficient structural reliability without an excessive reduction of the mechanical parameters used for the structural design.

2.2. Pore size distribution of unstabilised earth blocks

Fig. 2 shows the measured pore volume distribution of the same earth block material after various pre-conditioning measures. The porosity at 23 °C and 50 % RH is around 160 mm^3g^{-1}. Vacuum drying at 40 °C increases the porosity by around additional 20 mm^3g^{-1} and again by around 20 mm^3g^{-1} when drying at 105 °C. Nevertheless, the overall shape and trend of the three curves remain the same. Based on these experiments, a volume increase of specific pore diameters is not indicated. On the contrary, it indicates that the entire pore network is affected fairly homogenously and the pore volume distribution is shifted by a constant factor.

This quantification is crucial for further analyses. Taking chemisorption into account as illustrated in Fig. 4, one needs a quantitative relation how the pore network evolves due to chemisorption at different material moisture levels. If this is reduced to a constant factor for all pore diameters, the model complexity would significantly decrease.

2.3. Experimental sorption isotherm and adsorption theory

Fig. 3 shows the experimentally determined sorption isotherms of extruded and hand-moulded earth blocks. The samples were dried in a desiccator at 23 °C and 0 % RH. More details of the used devices for measuring the sorption isotherms and an overview of the used grain fractions are discussed in [1].

Besides experimental approaches, the sorption isotherm can also be predicted by the sorption theory. Based on the well-known Brunauer-Emmett-Teller (BET) sorption theory, multilayer adsorption on flat surfaces is modelled [9]. In case of small pore with pore radii in the low nanometre range, the variation of the Gibbs free energy due to the curvature of the adsorbed water film must be considered. This was done by Hillerborg by combining the BET theory with the Kelvin equation [10]. This effect is significant especially for *meso*-pores [11]. Nevertheless, a pore geometry must be assumed within this theoretical framework.

2.4. Reduced molecular diffusion due to the Knudsen effect

In partially saturated porous media, mass transfer can occur in two phases. In the liquid phase the mass balance is summarized by the hydraulic conductivity. In the gaseous phase it is expressed by the diffusion coefficient. Although we consider physisorption, in this study we focus only on the diffusive moisture transfer. One possible expression for diffusion in porous media is giving in the following equation [12 13].

$$q_v = \frac{\rho_{v,sat}\varphi D_0}{\omega}\int_{r_{min}}^{r_{max}} \frac{dV}{1+N_k} div(h) \qquad with\, N_k = \frac{l_m}{2(r-t_a)}$$

Here, q_v in $kgm^{-2}s^{-1}$ is the water vapour flux, $\rho_{v,sat}$ in kgm^{-3} is the saturated water vapor density, φ is the open porosity, D_0 in m^2s^{-1} is the water vapour diffusion coefficient in free atmosphere, and ω describes the tortuosity of the pore system. These parameters in front of the integral describe the molecular diffusion, while the integral accounts for the Knudsen effect. If the Knudsen number is $N_k \ll 1$, the integral reaches its maximum value of 1 and the effective gas diffusion is equal to the

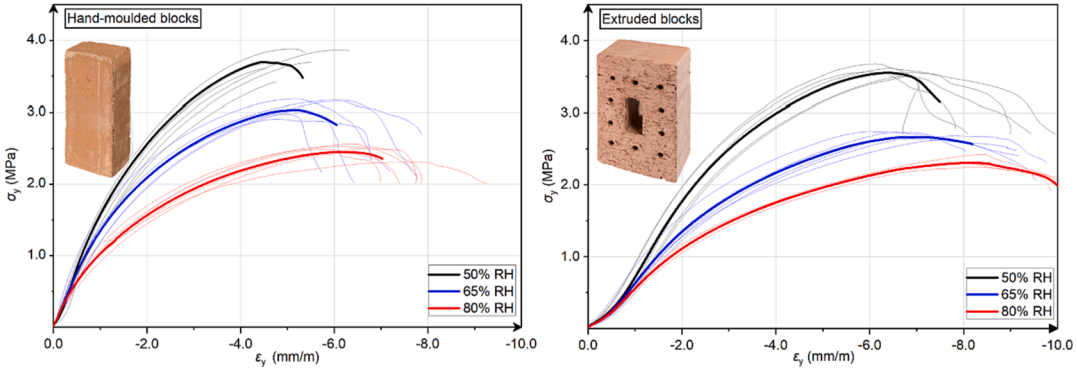

Fig. 1. Stress–strain relation of RILEM earth masonry specimens made from hand-moulded blocks (left) and extruded blocks (right) at varying RH; averaged curves of six specimens per masonry type and per RH.

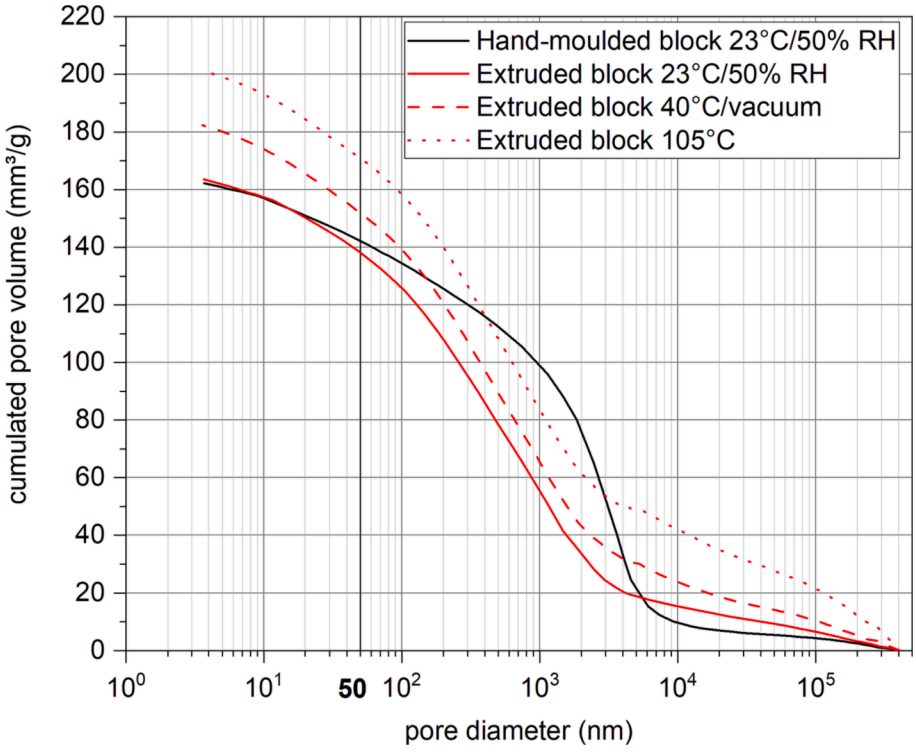

Fig. 2. Cumulative pore size distribution of earth blocks facing varying pre-treatment conditions.

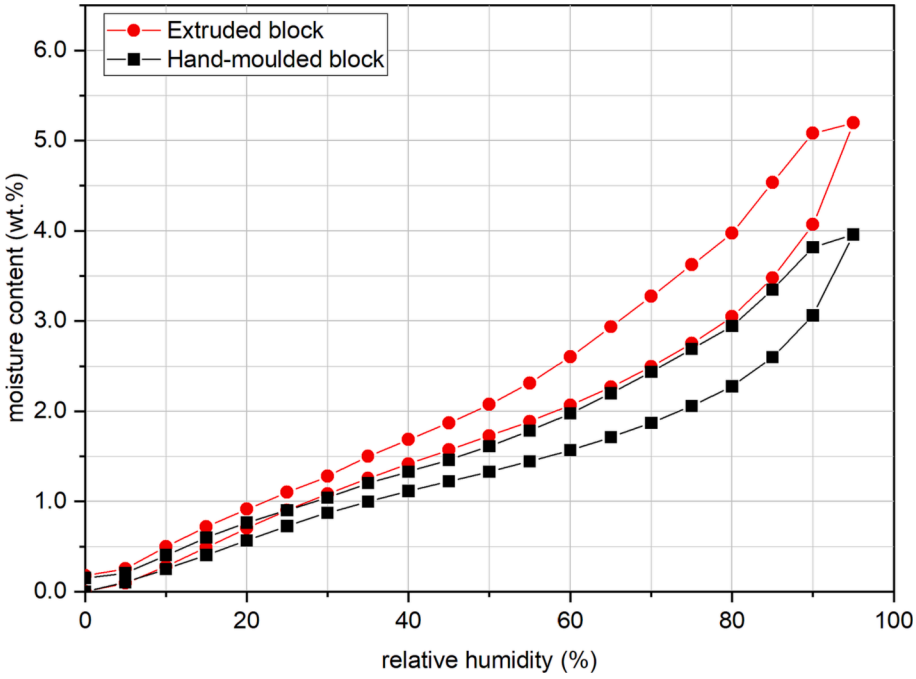

Fig. 3. Water vapour sorption isotherm of earth blocks at 23 °C.

molecular diffusion. If N_k is significantly above zero, the effective gas diffusion is reduced by the Knudsen effect. Here, l_m in m is the mean free path of air and t_a in m is the water layer, caused by physisorption. V is the normalised pore volume of the radius being considered and h is the relative humidity. A detailed discussion how physisorption might reduce molecular diffusion can be found in [14].

So far a stiff pore network is assumed, which has a constant porosity and pore volume distribution. On the contrary, clay minerals are known for chemisorption which leads to macroscopic swelling or shrinkage of the material (see Fig. 2). If sorption of the interlayer water changes the material dimensions, it probably affects the pore network and its moisture transport as well [15].

The Knudsen effect is visualized in a schematic sketch in Fig. 4. The initially pore confinement in dry state already reduces molecular diffusion as a molecule (red dot) performs not only collisions with other molecules (marked by red crosses), but it also interacts with the pore

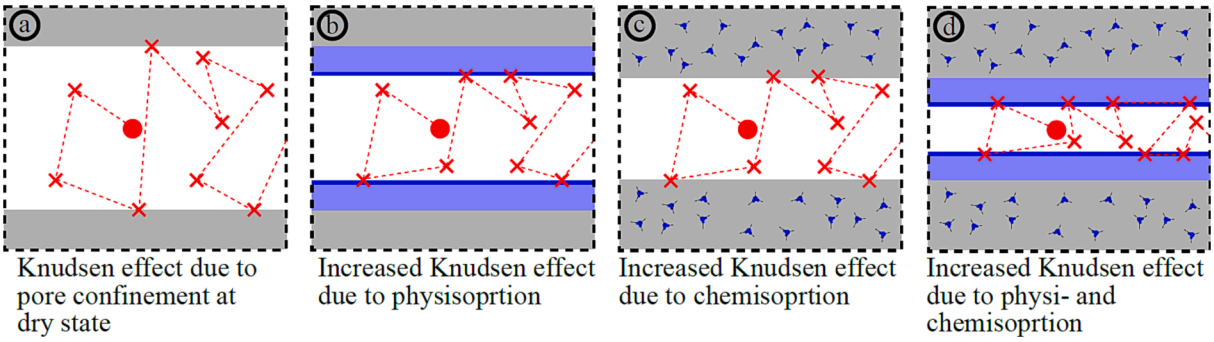

Fig. 4. Schematic sketch of molecular and Knudsen diffusion including chemisorption and physisorption.

wall. If physisorption occurs, the free pore space is further reduced by the adsorbed water layer, which makes collisions between the molecule and the confinement (in this case the liquid water layer) more likely. The same might occur in case of chemisorption. The solid material increases its volume by incorporating chemically bound water. This reduces the free pore space as well, leading to an increased number of molecule-pore wall collisions. If both effects occur simultaneously, even more pore space is occupied, and molecular diffusion is reduced further. This process can be analogously adapted to other chemisorption reactions such as carbonation, delayed ettringite formation, etc. as well as other (even inert) gases such as oxygen, carbon dioxide, etc.

3. Experimental setup

3.1. Experimental investigation of a free-standing earth masonry wall

The setup of the moisture monitoring of the earth masonry wall is shown in Fig. 5. The wall is exposed to outdoor climate conditions, but protected from direct weathering, which of course must be avoided in case of unstabilised earth masonry. Three measurement points were chosen for the humidity sensors. Each measurement point was equipped with two sensor-arrays. The arrays were embedded one from each side and adjusted in such a way that both inner sensors of each array are located exactly in the centre of the wall's cross section, whereas the outermost sensor is located ~ 12 mm outside the wall (Fig. 5 E). As a result, 15 measurement values per measurement point are available. The sensor spacing is more tightly close to the surface (distance d = 5 mm) and subsequently increases towards the centre (d = 2 – 4 cm). To ensure valid measurements, the data of the sensors outside the wall are compared to data obtained from the Deutsche Wetterdienst (DWD) recorded at BAM and the data obtained by the two sensors in the centre of the cross section are compared to each other. Additionally, a dryly core-drilled cylindric specimen (d = 40 mm) was extracted and measured by means of nuclear magnetic resonance in order to validate the measurement values.

3.2. Embedded sensor arrays

Fig. 5C and D show the embedded sensor arrays and the corresponding spacing. Five sensors have a separated casing, and four sensors are placed together in one casing to enable a tight spacing of 5 mm. In the combined casing, every sensor has its own separated chamber to avoid internal water vapor transport. Furthermore, every sensor is covered by a hydrophobic, porous membrane. This enables water vapor exchange between the sensor and the surrounding material whilst protecting the sensor from direct contact with water or clay during casting.

The drilled hole in the earth blocks had a diameter of 32 mm. The material used for filling the hole was the same as it was used for the original blocks. Therefore, the material and moisture transportation properties should be very similar and representative for the wall

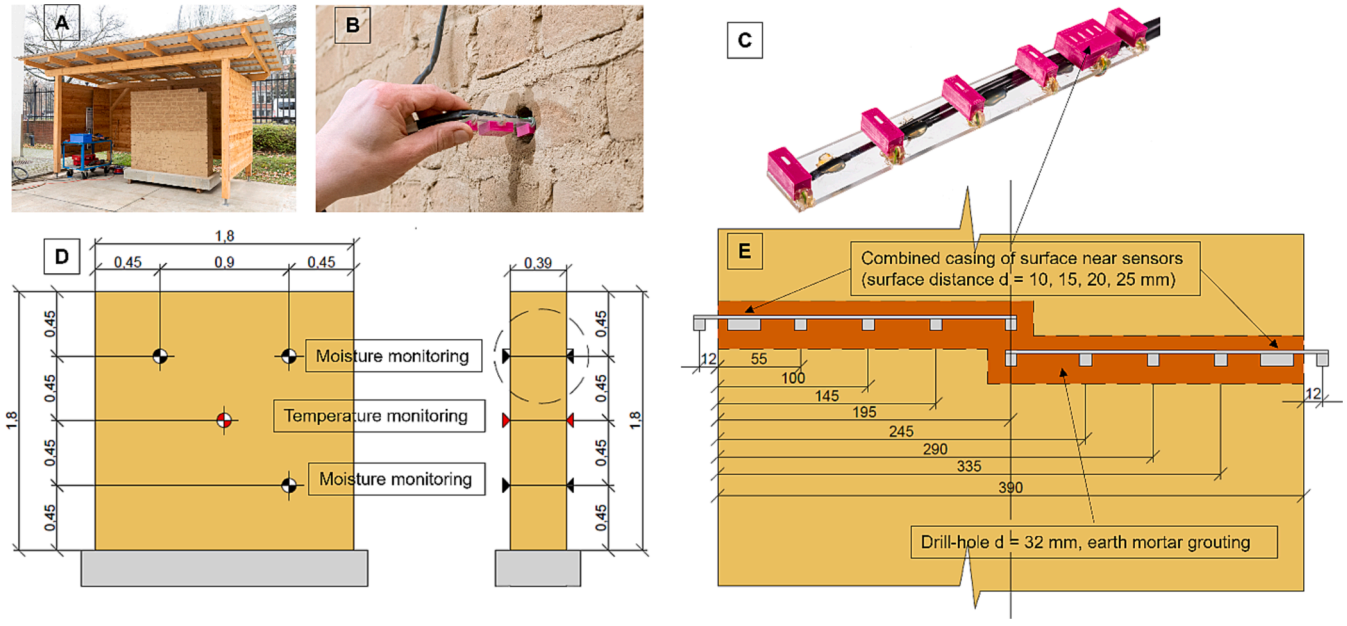

Fig. 5. Experimental setup of the moisture monitoring; A: Sheltered location of the experimental setup; B: Installation of a sensor array; C: Sensor array; D: Sketch of the measurement points; E: Detailed sketch of the alignment and spacing of the sensors.

material. The used relative humidity sensors were HIH-5030. To correct for temperature changes, also two PT100 temperature sensors were embedded into the wall. After installation, all sensors, expect one, were sending reasonable values. Using the same sensors in similar casings embedded into concrete are discussed in detail in [16,17].

4. Results and discussion

4.1. Moisture distribution of earth masonry exposed to outdoor climate conditions

Fig. 6 shows the measured maximum and minimum humidity inside the wall over almost one year. The highest variations of around 45 % to 95 % RH can be seen at the wall surface. These values are expected and within the range of average relative humidity in Berlin over the last 30 years with around 85 % RH in winter season and 65 % RH in summer season. Furthermore, the surface oriented south towards the sun shows slightly lower values. This is caused by a higher material temperature due to solar rays which heat up the surface and reduce the relative humidity in the pore network. The higher the distance to the surface, the lower the variations. At distances above 10 cm, the total humidity range is between 60 % RH and 80 % RH all year.

For four distinct humidity sensors at different depths, the measured humidity over one year is shown. As expected, the highest humidity values are recorded during winter season at all positions and the drier values in summer season. For the latter phase, one could assume that the moisture transport at humidity levels below 70 % RH takes place only in gaseous phase [18]. To derive the diffusion coefficient, the mass balance needs to be solved, whereas the pore saturation has to be known as well. For this, Hillerborg's adsorption theory is applied to the measured pore volume distribution [10]. Within this theoretical approach, a pore geometry needs to be assumed.

Different pore geometries possess different pore wall curvatures and hence lead to different pore saturations. The computation is presented in Fig. 7. In the range between 40 % RH and 90 % RH, a spherical pore geometry shows the highest correlation to the measured values. The sorption isotherms are comparable to other experimental studies [19 20 21]. The physisorbed water layer t_a is now determined and the corresponding reducing of available pore space. In conclusion, all required parameters are known to predict the influence of physisorption on the diffusion coefficient. Nevertheless, the underlying pore volume distribution was measured at dry state and do not incorporate chemisorption.

4.2. Quantitative assessment of the hygric expansion based on climate change experiments

Chemisorption describes the chemical absorption of water. On the

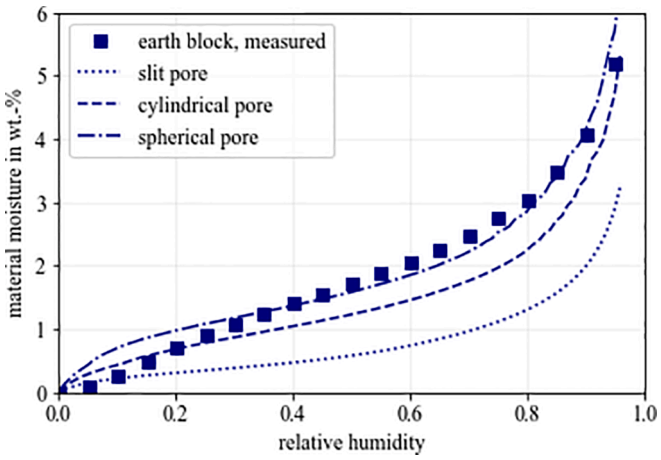

Fig. 7. Experimental and theoretical sorption isotherm for the earth block and for different pore geometries.

macroscopic scale, this effect is known as material swelling. Tests at different material moisture states were carried out for both used masonry materials to quantify this effect. Fig. 8 shows the measured axial strain of RILEM earth masonry specimens under usual service load for three cycles of humidity variation from 50 % RH to 65 % RH. Each adsorption or desorption cycle was done for seven days. However, we analyse only the first increase of relative humidity in the following because this represents pure adsorption without any hysteresis effects. Although full steady-state conditions are not reached after seven days, the slope is already monotonically decreasing. After the third cycle, the corresponding strain value would be around 25 % higher. However, for a first estimate, the measured strain is between 0.14 mm/m or 0.19 mm/m for a variation of 15 percentage points in relative humidity. As a first rough estimation, we assume a strain rate due to chemisorption of 0.01 mm/m for one percentage point variation in humidity. This strain rate is used for an estimation of the evolution of the pore volume distribution due to chemisorption.

4.3. Moisture distribution of earth masonry exposed to outdoor climate conditions

Macroscopic strain rates do not necessarily represent the variation of pore volume distribution as the solid material matrix itself exhibits elasto-plastic material behaviour. However, as a conservative assumption we postulate that the pores on microscopic scale are affected by the same strain rate of 0.01 mm/m for one percentage point of humidity variation. In fact, a pore of 1000 nm in diameter facing an increase of

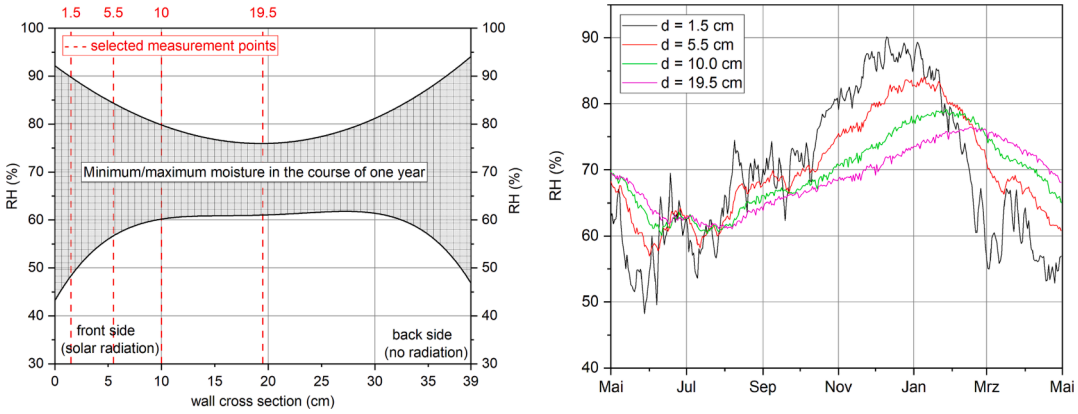

Fig. 6. Minimum and maximum values of the moisture distribution throughout the walls cross section (left) and development of the moisture content for selected measurement points in the period of one year.

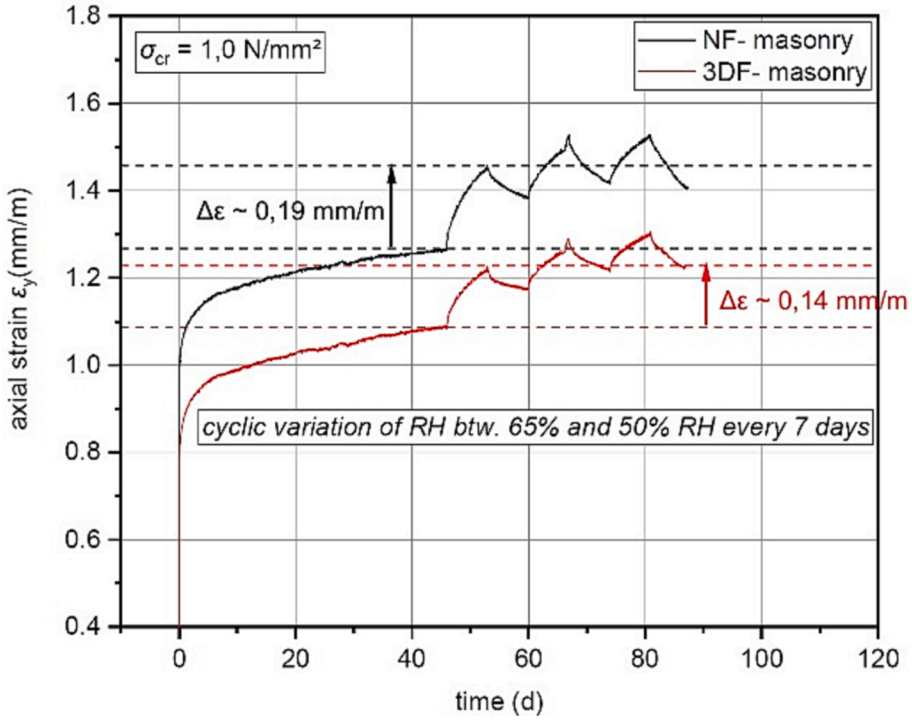

Fig. 8. Hygric expansion of the two masonry materials for cyclic material moisture variations.

one percentage point of humidity would be reduced to 999.99 nm. Three different pore sizes are analysed in Table 1 for three different humidity levels. The radius of the resulting air bubble in the centre of the spherical pore is r_{free} as only in this part of the pore diffusion can occur. The dry state can be considered as the baseline because it describes the Knudsen effect due to the pore confinement. For the smallest pore, this effect is obviously the greatest one and molecular diffusion is reduced the most. This is the stiff radius for the computation of the physisorbed water predicted by Hillerborg's adsorption theory, called here "only physisorption". For the smallest pore, only at 45 % RH a free space exists and for the two high humidity levels, full saturation is already reached. The case "only chemisorption" considers only the pore radius reduction due to the case by chemisorption without any adsorbed water layer. These two cases are just for comparison because physisorption and chemisorption will always occur simultaneously. The case "chemi- and physisorption" incorporates both effects simultaneously. First, we predicted the reduction of the initial sphere diameter with a strain rate of 0.01 mm/m for one percentage point of humidity variation. The new and thus slightly reduced diameter was then the input for the prediction of physisorption. As the adsorbed water layer thickness is a non-linear function of the pore radius, chemisorption must be considered before physisorption to account properly for the Kelvin effect. The resulting free radii were the input to compute the corresponding Knudsen number based on a mean free path of $l_m = 66.35$ nm.

Table 1
Free pore space and Knudsen number for different physi- and chemisorption states for spherical pores.

Initial spherical pore diameter	$r = 3.5$ nm		$r = 25$ nm		$r = 50$ nm	
Pore properties	r_{free}	N_K	r_{free}	N_K	r_{free}	N_K
Dry state	3.5 nm	9.48	25 nm	1.33	50 nm	0.66
45 % RH only physisorption	2.37 nm	14.02	24.39 nm	1.36	49.4 nm	0.67
65 % RH only physisorption	0 nm	—	23.94 nm	1.39	48.99 nm	0.68
85 % RH only physisorption	0 nm	——	21.77 nm	1.52	47.35 nm	0.7
45 % RH only chemisorption	3.4984 nm	9.48	24.9887 nm	1.33	49.9776 nm	0.66
65 % RH only chemisorption	3.4977 nm	9.48	24.9838 nm	1.33	49.9676 nm	0.66
85 % RH only chemisorption	3.497 nm	9.49	24.9786 nm	1.33	49.9575 nm	0.66
45 % RH chemi- and physisorption	2.36 nm	14.04	24.38 nm	1.36	49.38 nm	0.67
65 % RH chemi- and physisorption	0 nm	—	23.93 nm	1.39	48.96 nm	0.68
85 % RH chemi- and physisorption	0 nm	—	21.75 nm	1.53	47.31 nm	

4.4. Application for earth masonry

The standard EN 1015 for water vapour permeability considers only steady-state conditions and is in consequence not representative for dynamic situation [22]. In varying ambient conditions, thermal diffusion highly influences moisture transport [23]. Depending on the earth material, at humidity levels of roughly 75 % RH, water vapour diffusion and hydraulic conductivity interact with each other. This increases the complexity of moisture transport prediction [18,20]. Furthermore, in case of desorption, inkbottle water causes strong hysteresis effects in material moisture [17,24].

However, moisture transfer in earth masonry is of crucial importance for the load-bearing capacity [8] and for moisture buffering [25]. With increasing moisture content within the hygroscopic range, the compressive strength reduces by more than 60 % for earth material [3 21] and by 48 % for polymer modified earth material [25]. For the prediction of moisture buffering, better input parameters are required to meet building regulations in respect to thermal insulation [26]. Although several types of moisture transfer can be simulated with heat air moisture (HAM) models, they all rely on the investigated material and its pore network [27 28]. To increase moisture buffering, the moisture capacity can be increased by using more active clay minerals, but this also increases swelling and shrinkage [20].

Within the hygroscopic range, around 80 % of the material moisture is located in mesopores [11]. With the appearance of a physisorbed water film, adsorbed interlayer water and physisorbed capillary water, Lin et al. identified three types of water relevant for earth material. Furthermore, they speculated that clay swelling/chemisorption of water might have a great influence on the pore structure and, finally, on moisture transport [15]. The results in Table 1 show that the influence of chemisorption is negligible compared to physisorption in respect to water vapour gas diffusion in mesopores, including the Knudsen effect. Thus, the influence of swelling/shrinkage on gas diffusion can be ignored. This significantly reduces complexity as analytical models or simulations do not need to couple the water vapour diffusion coefficient with the local moisture content which would influence the locally available pore space. In conclusion, the pore network can be considered as rigid. Therefore, physisorption remains as the relevant influence for gas diffusion in partially saturated pores. Following Lin at al. [15], multilayer adsorption and capillary condensation need to be considered in more detail, including point-symmetric [11] and not point-symmetric [20] pore geometries. In future, further analysis of the moisture content of earth material can be validated by nuclear magnetic resonance measurements [29].

5. Conclusion

A free-standing earth masonry wall was equipped with six sensor arrays and every array consists of 9 humidity sensors in different depths. With this setup, the entire 40 cm wall was monitored over one year. The recorded data show reasonable trends with higher moisture at winter season and low humidity levels during summer season. Furthermore, sensors at higher depths record a smoother behaviour with fewer peaks.

Sorption theory was applied to the measured pore volume distribution and the highest correlation with experimental sorption isotherms was found for spherical pore geometries. Based on this, for every humidity level and pore size, the pore saturation and the physisorbed water film can be predicted. Furthermore, pore volume distributions of different pre-conditioning material samples indicated a homogenous increase in pore volume for all pore radii. This indicates that every pore size is affected similarly by chemisorption. Thus, we assumed a constant strain rate for every pore of 0.01 mm/m for one percentage point of humidity variation based on axial strain. Finally, we compute the free pore space and the Knudsen number for pure physisorption, pure chemisorption, and both effects occurring simultaneously.

For all analysed pore radii between 3.5 nm and 50 nm, the effect of chemisorption of the Knudsen number is negligible. Even for the smallest pore, which shows the strongest effects, chemisorption causes less than 1 % of the variation of the Knudsen number. The entire process is highly dominated by physisorption. As chemisorption does not influence noticeably the Knudsen number it will not have any influence on the molecular diffusion coefficient. This will simplify moisture transfer calculations for life cycle analysis [30] and buffering capacity [31].

Author contribution

Conception and creation of the entire text and all figures as well as proofreading (including references) are free of artificial intelligence based software or large language models. All content is generated by humans.

All authors have contributed substantially to the work reported in this publication. Conceptualization: C.S. and P.W.; methodology: C.S. and P.W.; software: C.S., H.S. and P.W.; validation: C.S. and P.W.; formal analysis: C.S. and P.W.; experimental setup: C.S., H.S. and P.W.; data recording: P.W.; data curation: C.S. and P.W.; resources: C.S., H.S. and P.W.; writing - original draft preparation: C.S.; writing - review and editing: C.S. and P.W.; visualization: C.S. and P.W.; supervision: C.S. and P.W. All authors have read and agreed to the published version of the manuscript.

CRediT authorship contribution statement

Christoph Strangfeld: Conceptualization, Data curation, Formal analysis, Investigation, Methodology, Resources, Software, Validation, Visualization, Writing – original draft, Writing – review & editing. **Heiko Stolpe:** Investigation, Resources, Software. **Philipp Wiehle:** Visualization, Validation, Methodology, Investigation, Data curation, Conceptualization, Resources, Software, Writing – review & editing.

Declaration of Competing Interest

We declare no competing interests. This study received no funding.

Data availability

Data will be made available on request.

References

[1] F. Ávila, E. Puertas, R. Gallego, Characterization of the mechanical and physical properties of unstabilized rammed earth: A review, Constr. Build. Mater. 270 (2021), 121435, https://doi.org/10.1016/j.conbuildmat.2020.121435.
[2] G. Minke, Building with earth: design and technology of a sustainable architecture, De Gruyter (2006), https://doi.org/10.1007/3-7643-7873-5.
[3] P. Wiehle, S. Simon, J. Baier, L. Dennin, Influence of relative humidity on the strength and stiffness of unstabilised earth blocks and earth masonry mortar, Constr. Build. Mater. 342 (2022), 128026, https://doi.org/10.1016/j.conbuildmat.2022.128026.
[4] P. Wiehle, M. Brinkmann, Material behaviour of unstabilised earth block masonry and its components under compression at varying relative humidity, Case Stud. Constr. Mater. 17 (2022) e01663.
[5] Vatani Oskouei, A. et al.: "Experimental investigation on mud bricks reinforced with natural additives under compressive and tensile tests," *Construction and Building Materials*, Article 142, pp. 137-147, 07/01/July 2017, doi: 10.1016/j.conbuildmat.2017.03.065.
[6] I. Aksu, E. Bazilevskaya, Z. T. Karpyn. Swelling of clay minerals in unconsolidated porous media and its impact on permeability. *GeoResJ*, 7: pp.1 -13. doi: 10.1016/j.grj.2015.02.003.
[7] P. Wiehle, M. Brinkmann. Load-bearing capacity of earth masonry – an experimental and numerical analysis. *LEHM 2020 - Proceedings*, Weimar, Germany.
[8] M. Brinkmann, P. Wiehle, Correlation between relative humidity and the strength and deformation characteristics of unstabilised earth masonry, Constr. Build. Mater. 366 (2023), 130048, https://doi.org/10.1016/j.conbuildmat.2022.130048.
[9] S. Brunauer, P.H. Emmett, E. Teller, Adsorption of gases in multimolecular layers, J. Am. Chem. Soc. 60 (2) (1938) 309–319, https://doi.org/10.1021/ja01269a023.
[10] A. Hillerborg, A modified absorption theory, Cem. Concr. Res. 15 (5) (1985) 809–816, https://doi.org/10.1016/0008-8846(85)90147-4.
[11] C. Strangfeld, P. Wiehle, S.M. Munsch, About the dominance of mesopores in physisorption in amorphous materials, Molecules 26 (7190) (2021) 1–22, https://doi.org/10.3390/molecules26237190.
[12] T. Ishida, K. Maekawa, T. Kishi, Enhanced modeling of moisture equilibrium and transport in cementitious materials under arbitrary temperature and relative humidity history, Cem. Concr. Res. 37 (4) (2007) 565–578, https://doi.org/10.1016/j.cemconres.2006.11.015.
[13] K. Maekawa, R. Chaube, T. Kishi, Modelling of concrete performance, E & FN Spon, London, 1999.
[14] C. Strangfeld, Quantification of the Knudsen effect on the effective gas diffusion coefficient in partially saturated pore distributions, Adv. Eng. Mater. (2021), https://doi.org/10.1002/adem.202100106.
[15] X. Lin, Q. Hu, Z. Chen, Q. Wang, T. Zhang, M. Sun, Changes in water vapor adsorption and water film thickness in clayey materials as a function of relative humidity, Vadose Zone J. 19 (1) (2020) e20063.
[16] C. Strangfeld, S. Johann, M. Bartholmai, Smart RFID sensors embedded in building structures for early damage detection and long-term monitoring, Sensors 19 (24) (2019) 1–18, https://doi.org/10.3390/s19245514.
[17] C. Strangfeld, S. Kruschwitz, Monitoring of the absolute water content in porous materials based on embedded humidity sensors, Constr. Build. Mater. 177 (2018) 511–521, https://doi.org/10.1016/j.conbuildmat.2018.05.044.
[18] C. Strangfeld, Determination of the diffusion coefficient and the hydraulic conductivity of porous media based on embedded humidity sensors, Constr. Build. Mater. 263 (2020) 1–13, https://doi.org/10.1016/j.conbuildmat.2020.120092.
[19] A. Arrigoni, A.-C. Grillet, R. Pelosato, G. Dotelli, C.T. Beckett, M. Woloszyn, D. Ciancio, Reduction of rammed earth's hygroscopic performance under stabilisation: an experimental investigation, Build. Environ. 115 (2017) 358–367, https://doi.org/10.1016/j.buildenv.2017.01.034.
[20] F. McGregor, A. Heath, A. Shea, M. Lawrence, The moisture buffering capacity of unfired clay masonry, Build. Environ. 82 (2014) 599–607, https://doi.org/10.1016/j.buildenv.2014.09.027.

[21] F. El Fgaier, Z. Lafhaj, C. Chapiseau, E. Antczak, Effect of sorption capacity on thermo-mechanical properties of unfired clay bricks, J. Build. Eng. 6 (2016) 86–92, https://doi.org/10.1016/j.jobe.2016.02.011.

[22] EN 1015-19 Methods of test for mortar for masonry - part 19: Determination of water vapour permeability of hardened rendering and plastering mortars. *European standard*, 1998.

[23] K. Abahri, R. Belarbi, and A. Trabelsi. Contribution to analytical and numerical study of combined heat and moisture transfers in porous building materials. Building and Environment, 46(7):1354–1360, 2011. doi: 10.1016/j.buildenv.2010.12.020.

[24] B. Libby, P.A. Monson, Adsorption/desorption hysteresis in inkbottle pores: a density functional theory and Monte Carlo simulation study, Langmuir 20 (10) (2004) 4289–4294, https://doi.org/10.1021/la036100a.

[25] A.M. Amde, J.V. Martin, J. Colville, The effect of moisture on compressive strength and modulus of brick masonry. Proceedings of the 13th International Brick and Block Masonry Conference, 2004.

[26] S. Goodhew, R. Griffiths, Sustainable earth walls to meet the building regulations, Energ. Build. 37 (5) (2005) 451–459, https://doi.org/10.1016/j.enbuild.2004.08.005.

[27] S. Dubois, F. McGregor, A. Evrard, A. Heath, F. Lebeau, An inverse modelling approach to estimate the hygric parameters of clay-based masonry during a moisture buffer value test, Build. Environ. 81 (2014) 192–203, https://doi.org/10.1016/j.buildenv.2014.06.018.

[28] M. Labat, C. Magniont, N. Oudhof, J.-E. Aubert, From the experimental characterization of the hygrothermal properties of straw-clay mixtures to the numerical assessment of their buffering potential, Build. Environ. 97 (2016) 69–81, https://doi.org/10.1016/j.buildenv.2015.12.004.

[29] M. Härder, Experimentelle und nummerische Untersuchungen zum Feuchteverhalten tragender Lehmbaustoffe, Technische Universität München, 2021. Master thesis.

[30] A. Arrigoni, C. Beckett, D. Ciancio, and G. Dotelli. Life cycle analysis of environmental impact vs. durability of stabilised rammed earth. *Construction and Building Materials*, 142:128–136, 2017. doi:10.1016/j.conbuildmat.2017.03.066.

[31] C. Rode, R. Peuhkuri, B. Time, K. Svennberg, and T. Ojanen. Moisture buffer value of building materials. *Journal of ASTM International*, 4(7):1–13, 2007. doi:10.1520/stp45403s.